Possibility to form $Z = 120$ via the $^{64}Ni + ^{238}U$ reaction using the dynamical cluster-decay model

Sahila Chopra,[1] Manoj K. Sharma,[2] Peter Oto Hess,[3] and Jasleen Bedi[1]
[1]*Department of Physics, Panjab University, Chandigarh 160014, India*
[2]*School of Physics and Material Science, Thapar University, Patiala 147004, India*
[3]*Instituto de Ciencias Nucleares, UNAM, 04510 Mexico City, Mexico*

(Received 5 November 2021; accepted 20 December 2021; published 14 January 2022)

According to different theoretical studies, the next magicity for the proton number should occur at $Z = 114$, 120, or 126 and for the neutron number $N = 184$. Superheavy nuclei of interest for the forthcoming synthesis of the isotopes with $Z = 119$, 120 are investigated. Many reactions have yet to be studied in order to find the possible incoming channels for the formation of $Z = 120$. In this work, synthesis of superheavy element 120 in terms of the fission and quasifission cross sections via $^{64}Ni + ^{238}U$ reaction is evaluated and discussed. We have explored the possibility of formation of $Z = 120$ via $^{64}Ni + ^{238}U$ reaction, using the experimental data from Kozulin *et al.*, Phys. Lett. B **686**, 227 (2010). Some experimental efforts have been made to synthesize $^{302}120$, via Ni-induced and Cr-induced reaction, i.e., $^{64}Ni + ^{238}U$ reaction at five E^*'s (excitation energies) and the $^{54}Cr + ^{248}Cm$ reaction at only one energy, respectively. In this work, we have studied the Ni-induced reaction at given energies by including higher multipole deformations $\beta_{\lambda i}$ ($\lambda = 2, 3, 4$; $i = 1, 2$), and compact orientations θ_{ci} using the coplanar degree of freedom ($\Phi = 0^\circ$) within the framework of the dynamical cluster-decay model (DCM). The neck-length parameter is the only one, which is fixed in reference to the observed data for fission cross section (σ_{ff}) calculated for mass region $A/2 \pm 20$, and quasifission cross section (σ_{qf}) for the incoming channel of $^{64}Ni + ^{238}U$ reaction. Our calculations for Ni-induced reaction have shown a good concurrence with the experimental data for quasifission and fission cross sections along with the DCM-calculated estimated and predicted cross sections for evaporation residues (ERs), which can be used for future references. Our results demonstrate the insignificant compound nucleus formation possibility P_{CN} ($\ll 1$) for $Z = 120$ from Ni-induced reaction because of the very low order of evaporation residues; thus, this work is not supporting this incoming channel for the formation of $Z = 120$.

DOI: 10.1103/PhysRevC.105.014610

I. INTRODUCTION

Over the past few years, much progress has been made in the production and investigation of superheavy elements (SHE). Presently the main interest of nuclear scientists is to synthesize $Z = 119$ and 120 elements. The heaviest known element, $Z = 118$, oganesson (after scientist Yuri Oganessian), was observed in 2002, later independently confirmed, and given an official name in 2016. We have used the dynamical cluster-decay model (DCM) for the analysis of $Z = 120$ via $^{64}Ni + ^{238}U$ reaction at five E^*'s of 19, 23, 31, 43, and 62 MeV from Ref. [1] and besides some comparative analysis for $^{54}Cr + ^{248}Cm$ reaction using the DCM. Here, to understand the superheavy element (SHE) production mechanisms, we are working on the theory which explains the extreme case, the nuclei fuse and a compound nucleus (CN) are formed. The CN de-excites by evaporating nucleons ("fusion evaporation" or ER) or by fission ("fusion fission" or ff). The nuclear system can also reseparate before CN formation, thus resulting in quasifission (qf). The capture cross section or total fusion cross section is then the sum of qf, ff, and ER cross sections: $\sigma_{fusion} = \sigma_{qf} + \sigma_{ff} + \sigma_{ER}$. Experimentally, for Ni-induced reaction, fission (σ_{ff}) and quasifission (σ_{qf}) cross sections are measured. The experiments for Ni-induced reaction were performed at the Physics Department of the University of Jyväskylä using a ^{64}Ni beam from the cyclotron K-130. Another reaction of interest, $^{54}Cr + ^{248}Cm$, was investigated at the velocity filter the separator for heavy ion reaction products (SHIP), at Gesellschaft fuer Schwerionenforschung (GSI), Darmstadt, with the intention to study the production and decay properties of isotopes of element 120. We have also explored the possibility to form $Z = 120$ via Cr-induced reaction after taking an idea from Ref. [2], in which experimentalists are talking about the one event cross section for ERs. We have tried to calculate the ERs cross section, but we do not have any experimental evidence and is given so far that experimental results are used which themselves are not yet confirmed [2]. Experimentally, a complete decay chain cannot be established, so the evaporation residue cannot be identified, whereas three correlated signals were measured or one event cross section given as a limit, which occurred experimentally within a period of 279 ms. The one event cross-section limit from all three parts is $0.58^{+1.35}_{-0.48}$ pb (i.e., sensitivity of the experiment). We have just taken this value as a reference number as a limit and tried to test the number using the DCM. We have studied these reactions using the dynamical cluster-decay model (DCM) of Gupta and collaborators (see,

e.g., Refs. [3–6]). Ni-induced reaction has the fission region of $A = 123$–142, i.e., $A/2 \pm 20$, and we have calculated the estimated cross section for evaporation residues (ERs) at all energies. In the case of Cr-induced reaction for the fission region taken as ($A = 124$–142, i.e., $A/2 \pm 18$), we have tried to scrutinize the cross section for the evaporation residues. Further experiments are called for.

For the $^{64}\mathrm{Ni} + ^{238}\mathrm{U}$ reaction, we have compared our DCM-calculated cross sections for σ_{ff} and σ_{qf} at all given center-of-mass energies E^*'s with the experimental data. We have studied this reaction within the framework of the DCM along with the set of parameters: coplanar degree of freedom $\Phi = 0^0$, higher multipole deformations $\beta_{\lambda i}$ ($\lambda = 2, 3, 4$; $i = 1, 2$), and compact orientations θ_{ci}. We have also calculated the cross sections for unobserved evaporation residues (ERs) at all energies as we have done in our previous work for the case of $Z = 122$ [5]. For $Z = 120$, we are more interested to find or predict the ERs cross section because the compound nucleus fusion probability (P_{CN}) mainly depends on the formation of evaporation residues and gives a pretty good idea of the process of fusion. Our calculated results are in agreement with the experimental data for the fission (ff) and quasifission (qf) cross sections. In this work, we have also mentioned the possible target-projectile (t-p) combinations. Another point of interest for $Z = 120$, is the neck-length parameter (ΔR) in the case of ERs ($1n$–$4n$), which becomes automatically the same during our calculations at all energies. However, for $Z = 122$, we have taken the same ΔR "intentionally" (see Ref. [5]). In both cases, $Z = 122$ and 120, the estimated cross sections of the evaporation residues are of the order of picobarn (pb). We found for $Z = 120$, the largest contribution of $1n$ and lowest for $4n$ decay channels. Different nuclear models contain a number of parameters to study the different aspects of the nuclear reactions which are fixed for the best description of known nuclei. Here, we have also a realistic parameter ΔR, as we have discussed the ability of this parameter to predict the cross section of unobserved decay fragments in our published works (see, e.g., Refs. [5] and [7]). Therefore, our calculations have provided valid results which need further experimental confirmation. We have also calculated the compound nucleus formation (fusion) and survival probability, P_{CN} and P_{surv} respectively. P_{CN} defines the formation of a dinuclear configuration formed at the minimum potential around the touching point: When two heavy ions are captured and the kinetic energy of their relative motion transferred into the potential and excitation energy. Next, the important quantity is P_{surv}: The survival probability defines the probability of the excited compound nucleus to reach the ground state by neutron emission. On the bases of these quantities we do not recommend $^{64}\mathrm{Ni} + ^{238}\mathrm{U}$ incoming channel to form $Z = 120$ (later explained).

The paper is organized as follows. Section II gives a brief description of the dynamical cluster-decay model (DCM). Our calculations for $^{64}\mathrm{Ni} + ^{238}\mathrm{U}$ reaction, using this set of parameters: coplanar degree of freedom, higher multipole deformations $\beta_{\lambda i}$ ($\lambda = 2, 3, 4$; $i = 1, 2$), and θ_{ci} are given in Sec. III. Finally, the summary and conclusions of our work are presented in Sec. IV.

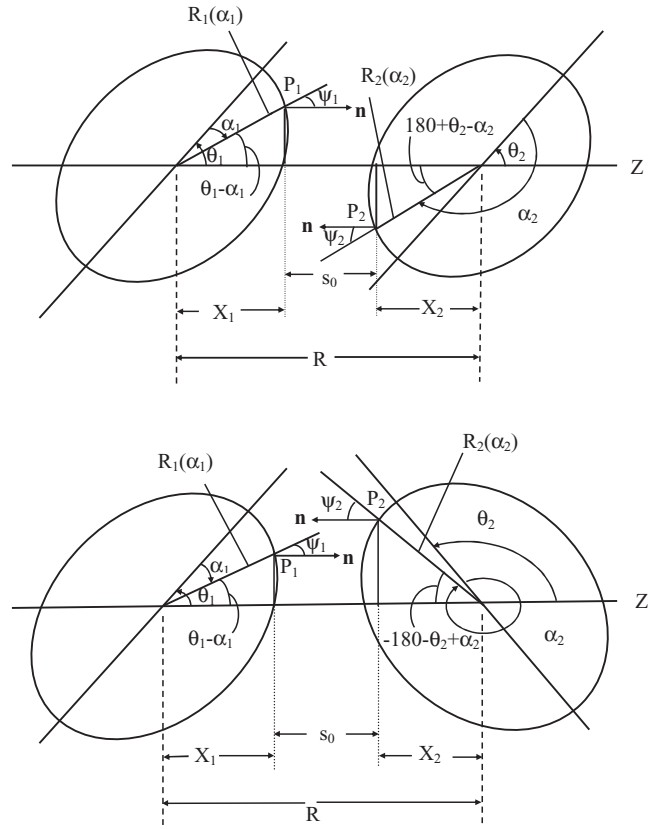

FIG. 1. Schematic configurations of two (equal or unequal) axially symmetric deformed, oriented nuclei, lying in the same plane and for various θ_1 and θ_2 values in the range 0° to 180°. The θ's are measured in anticlockwise from the colliding axis and the angle α's in clockwise from the symmetry axis (see Ref. [8]).

II. THE DYNAMICAL CLUSTER-DECAY MODEL (DCM)

The dynamical cluster-decay model (DCM) of Gupta and collaborators [4,6] is based on the dynamical or quantum mechanical fragmentation theory (QMFT), based on the two-center shell model (TCSM), used as an average two-body potential within the Strutinsky macro-microscopic method. This theory uses the collective coordinates of mass (and charge) asymmetries η (and η_Z) [$\eta = (A_1 - A_2)/(A_1 + A_2)$, $\eta_Z = (Z_1 - Z_2)/(Z_1 + Z_2)$], and relative separation R, with multipole deformations up to hexadecupole $\beta_{\lambda i}$ ($\lambda = 2, 3, 4$; $i = 1, 2$) and orientations θ_i. For the case of the colliding nuclei lying in the same plane $\Phi = 0$, Fig. 1 gives two best possible configurations of two (equal or unequal) nuclei separated by distance R and having any two (equal, unequal, acute, and obtuse) orientations θ_i. In addition, there are also the other configurations with orientations ($\theta_1 = 0°$, $\theta_2 = 180°$), ($\theta_1 = 0°$, $\theta_2 = 90°$) and ($\theta_1 = 90°$, $\theta_2 = 90°$). In terms of these coordinates, we define the compound nucleus decay cross section for ℓ partial waves as the compound nucleus decay or formation cross section of fragments for ℓ partial waves is defined in the DCM for each pair of exit and/or decay

channel:

$$\sigma_{(A_1,A_2)} = \frac{\pi}{k^2}\sum_{\ell=0}^{\ell_{\max}}(2\ell+1)P_0P;\;\; k=\sqrt{\frac{2\mu E_{\rm c.m.}}{\hbar^2}}, \qquad (1)$$

where P_0 is the fragment preformation probability, referring to the η motion at fixed R value, and P, the barrier penetrability, to R motion for each η value, both dependent on T and ℓ. The reduced mass $\mu = mA_1A_2/(A_1+A_2)$ with m as the nucleon mass. $\ell_{\max}$ is the maximum angular momentum, defined for light-particle evaporation residue cross section $\sigma_{\rm ER} \to 0$. Then, it follows from Eq. (1) that

$$\sigma_{\rm ER} = \sum_{A_2=1}^{4}\sigma_{(A_1,A_2)} \;\text{ or }\; = \sum_{x=1}^{4}\sigma_{xn}, \qquad (2)$$

and

$$\sigma_{\rm ff} = 2\sum_{A_2=5\text{ or }6}^{A/2}\sigma_{(A_1,A_2)}. \qquad (3)$$

The above equation is also applicable to the case where the ff process is measured in terms of so-called intermediate mass fragments (IMFs; $5 \leqslant A_2 \leqslant 20$, $3 \leqslant Z_2 \leqslant 10$) with the sum taken up to the maximum measured value of A_2 and without the multiplying factor 2. The same equation (1) is also applicable to the noncompound nucleus (nCN) decay process, calculated here as the quasifission (qf) and nCN decay channel, where $P_0 = 1$ for the incoming channel since the target and projectile nuclei can be considered to have not yet lost their identity. Then, for P calculated for the *incoming channel*$\eta_{\rm ic}$ is given by

$$\sigma_{\rm nCN} = \frac{\pi}{k^2}\sum_{\ell=0}^{\ell_{\max}}(2\ell+1)P_{\eta_{ic}}. \qquad (4)$$

Thus, using Eq. (1) in Eqs. (2) and (3), the DCM predicts not only the total fusion cross section $\sigma_{\rm fusion}$, i.e., the sum of the cross sections of constituents ER, ff, and nCN, but also includes the cross section of $\sigma_{\rm ER}$, $\sigma_{\rm ff}$, and $\sigma_{\rm nCN}$ channels. In Eq. (1), apparently, η and R motions are taken as decoupled, though in general they are coupled, as justified in Refs. [9–12], such that the stationary Schrödinger equation for the coupled η and R coordinates (with η_Z coordinate minimized, and hence kept fixed) is given by

$$H(\eta,R)\psi(\eta,R) = E\psi(\eta,R) \qquad (5)$$

with the Hamiltonian constructed as

$$H(\eta,R) = E(\eta)+E(R)+E(\eta,R) + V(\eta)+V(R)+V(\eta,R). \qquad (6)$$

Here, E refers to the kinetic energy (expressed in terms of mass parameters B_{ij}; $i,j = R,\eta$ [13–15]) and $V(\eta,R,T)$, the T-dependent collective potential energy calculated as per the Strutinsky renormalization procedure ($B = V_{\rm LDM}+\delta U$), using the T-dependent liquid drop model energy $V_{\rm LDM}(T)$ of Davidson *et al.* [16] with its constants at $T = 0$ refitted [17–19] to give the experimental binding energies of Audi *et al.* [20] and the "empirical" shell corrections δU of Myers and Swiatecki [21] for spherical nuclei, also made T dependent to vanish exponentially, added to T-dependent nuclear proximity V_P, Coulomb V_C, and ℓ-dependent potential V_ℓ for deformed, oriented nuclei. The temperature T (in MeV) is related to the CN excitation energy E^* ($= E_{\rm c.m.}+Q_{\rm in}$, with $Q_{\rm in}$ as the entrance channel Q value) as

$$E^* = (A/a)T^2 - T \;(T \text{ in MeV}),$$

with the level density parameter $a = 11$ for SHE (for others $a = 8$–9), depending on mass A of the CN. For V_P, we use the pocket formula of Blocki *et al.* [22]. The moment of inertia I is

$V_\ell(T)$ $[= \hbar^2\ell(\ell+1)/2I(T)]$ is either in the complete sticking limit $I = I_S(T) = \mu R^2 + \frac{2}{5}A_1mR_1^2(\alpha_1,T) + \frac{2}{5}A_2mR_2^2(\alpha_2,T)$ or, as used in experimental analysis, in the nonsticking limit $I = I_{\rm NS} = \mu R^2$. The angles α_i, $i = 1,2$, used to define the radius vectors R_i of deformed nuclei [see Eq. (9) below] are measured in a clockwise direction from the symmetry axis. For the kinetic energy part, the mass parameters $B_{\eta\eta}$ used are the smooth classical hydrodynamical masses [13]. Then, the Hamiltonian (5), for each ℓ value, on using the Pauli-Podolsky prescription [23], takes the form

$$H = -\frac{\hbar^2}{2\sqrt{B_{\eta\eta}}}\frac{\partial}{\partial\eta}\frac{1}{\sqrt{B_{\eta\eta}}}\frac{\partial}{\partial\eta} - \frac{\hbar^2}{2\sqrt{B_{RR}}}\frac{\partial}{\partial R}\frac{1}{\sqrt{B_{RR}}}\frac{\partial}{\partial R} + V(\eta)+V(R), \qquad (7)$$

The Schrödinger equation (5) becomes separable in η and R coordinates, whose solutions are $|\psi(\eta)|^2$ and $|\psi(R)|^2$, respectively, gives the probabilities P_0 and P of Eq. (1). The $P_0(A_i)$ is obtained at a fixed $R = R_a$, the first turning point(s) of the penetration path(s) for different ℓ values. Next, the penetrability P, instead of solving the corresponding radial Schrödinger equation in R, is given by the WKB (Wentzel, Kramers, and Brillouin) integral, which is solved analytically [24,25]. For more details, see Refs. [26,27].

In the decay of a hot CN, for R_a we use the postulate [18,19]

$$R_a(T) = R_1(\alpha_1,T)+R_2(\alpha_2,T)+\Delta R(\eta,T), = R_t(\alpha,\eta,T)+\Delta R(\eta,T), \qquad (8)$$

with radius vectors

$$R_i(\alpha_i,T) = R_{0i}(T)\left[1+\sum_\lambda \beta_{\lambda i}Y_\lambda^{(0)}(\alpha_i)\right] \qquad (9)$$

having temperature-dependent nuclear radii $R_{0i}(T)$ for the equivalent spherical nuclei [28],

$$R_{0i} = \left[1.28A_i^{1/3} - 0.76 + 0.8A_i^{-1/3}\right](1+0.0007T^2). \qquad (10)$$

Thus, R_a introduces a T-dependent parameter $\Delta R(T)$, the neck-length parameter, which assimilates the deformation and neck formation effects between two nuclei [29–31]. See Fig. 2: As ℓ value increases, the potential $V(R_a,\ell)$ increases, and hence R_a acts like a parameter through $\Delta R(\eta,T)$. We define R_a to have the same value for all ℓ values, since we do not know how to add the ℓ effects in binding energies. Note that ΔR introduces an in-built property of "barrier lowering" since each ℓ, $V(R_a,\ell)$ can be related to the top of the barrier

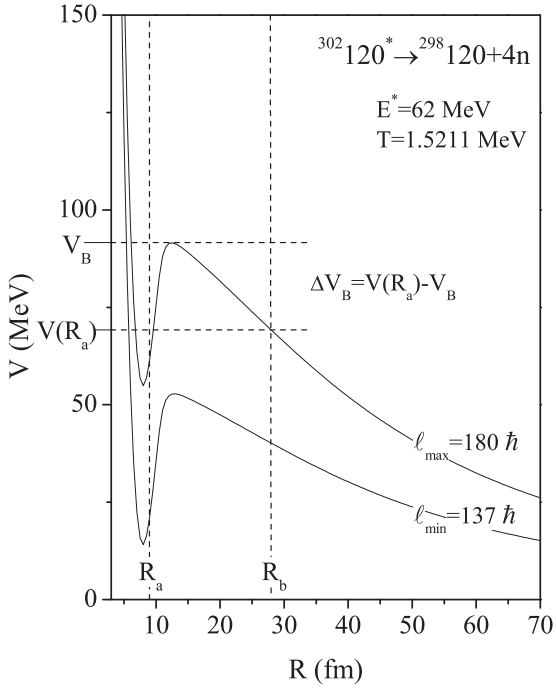

FIG. 2. Scattering potential $V(R)$ for $A_2 = 4n$, for $T = 1.5211$ MeV, at two different ℓ values ($\ell_{\min}$ and $\ell_{\max}$). The definition of "barrier lowering" $\Delta V_B(\ell) = V(R_a, \ell) - V_B(\ell)$ is also shown in this figure with $\ell = 180\hbar$.

$V_B(\ell)$ by defining $\Delta V_B(\ell) = V(R_a, \ell) - V_B(\ell)$ as the effective lowering of the barrier; i.e., the actually used barrier is effectively minimized [4,6].

Finally, the compound nucleus formation probability $P_{\rm CN}$ is defined as

$$P_{\rm CN} = \frac{\sigma_{\rm CN}}{\sigma_{\rm fusion}} = 1 - \frac{\sigma_{\rm nCN}}{\sigma_{\rm fusion}}, \tag{11}$$

and the compound nucleus survival probability $P_{\rm surv}$, the probability that the fused system will de-excite by emission of neutrons or LPs (equivalently, the ER) rather than fission, as

$$P_{\rm surv} = \frac{\sigma_{\rm ER}}{\sigma_{\rm CN}}, \tag{12}$$

where $\sigma_{\rm fusion} = \sigma_{\rm CN} + \sigma_{\rm nCN}$ and $\sigma_{\rm CN} = \sigma_{\rm ER} + \sigma_{\rm ff}$.

III. CALCULATIONS AND RESULTS

In this section, we present the result of our calculations for $Z = 120$, where the DCM-based fission $\sigma_{\rm ff}$ and quasifission $\sigma_{\rm qf}$ cross sections are in good agreement with the available experimental data at four excitation energies, i.e., $E^* = 19$, 31, 43, 62 MeV, but evaporation residues are not yet observed. We have calculated the estimated and predicted cross sections for evaporation residues (ERs), within the framework of the DCM. It is relevant to note that the (total) capture cross section in the case of superheavy elements (SHEs) is calculated as ($\sigma_{\rm capture} = \sigma_{\rm ER} + \sigma_{\rm ff} + \sigma_{\rm qf}$). We have done these calculations for the set of parameters: coplanar degree of freedom, higher multipole deformations $\beta_{\lambda i}$ ($\lambda = 2, 3, 4$; $i = 1, 2$), and compact orientations θ_{ci}. In these calculations, we have observed

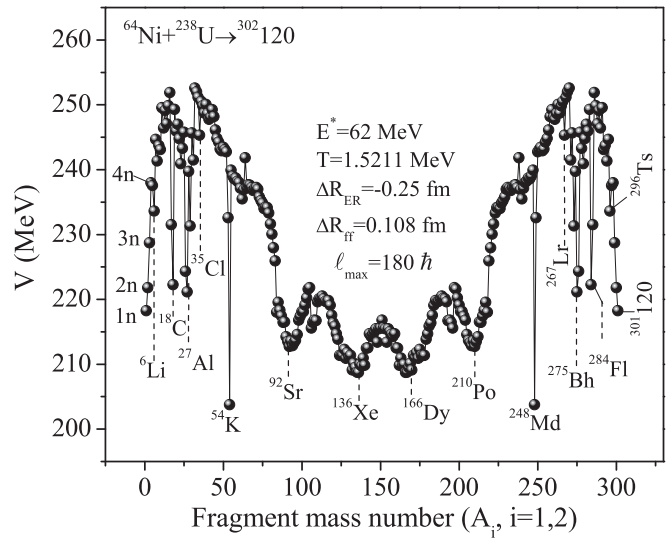

FIG. 3. Mass fragmentation potential minimized in charge-asymmetry coordinate η_Z for the decay of $^{302}120^*$ formed in $^{64}\mathrm{Ni} + ^{238}\mathrm{U}$ reaction at $E^* = 62$ MeV and at $\ell = 180\hbar$ values.

some interesting results regarding the neck-length parameter (ΔR) in the case of unobserved evaporation residues (ERs) (given in Table II), i.e., $\Delta R_{\rm ERs} = -0.25$ fm at all energies for $\sigma_{\rm ER}$ (ER = $1n$–$4n$). In this work, the evaporation residues are very low in production, of the order of 10^{-18} pb, which affects the compound nucleus formation or fusion probability $P_{\rm CN}$ of $Z = 120$ and concludes there is not the possibility to form a compound nucleus via $^{64}\mathrm{Ni} + ^{238}\mathrm{U}$ reaction, so we are not supporting this incoming channel for the formation of $Z = 120$.

Figure 3 shows the calculated mass fragmentation potential $V(A_2)$ for the best fitted ΔR values to both the measured ff and qf cross sections at $E^* = 62$ MeV ($T = 1.5211$ MeV), at $\ell_{\max}$ value (Fig. 4). This graph also tells us about the possible target-projectile combinations (t-p), which refers to the minimum potential energy surfaces (PES), and we would like to suggest these t-p combinations for the synthesis of $Z = 120$ (see Table I). According to Table I, these few t-p combinations (if experimentally possible and targets are stable) can be considered for the formation of $Z = 120$ and we would like to mention about the t-p combinations not to take, those which do not survive in our calculations using the DCM due to the reduced shell effects at the considered temperature and low binding energies of the incoming channels. In our calculations, the maximum yield P_0 is obtained for the measured symmetric fission ($A/2 \pm 20$) ($A = 123$–142) and for experimentally unobserved light particles ($A \leqslant 4$) we have calculated the estimated and predicted cross sections. The $\ell_{\max}$ and $\ell_{\min}$ values are fixed, respectively, via Figs. 4 and 5, where the calculated P_0 and P (using $V(\eta)$ in Fig. 3) are plotted as a function of ℓ for the illustrative ER channels and other decay fragments. For $\ell_{\max}$ and $\ell_{\min}$ values, the corresponding ER cross sections go to zero; i.e., the contributions of P_0 and P become negligible ($<10^{-10}$). As illustrated in Fig. 4, the $\ell_{\max}$ values for the two processes ER and ff are, respectively, fixed for $P_0 \rightarrow 0$ and becoming maximum with a (nearly) constant

TABLE I. This table showing the possible target-projectile (t-p) combinations (as shown in Fig. 3) higher-multipole deformations $\beta_{\lambda i}$ (λ=2,3,4; i=1,2). The probable decay fragments has fallen on the minimized potential energy surfaces and offered us the t-p combinations for the formation of Z=120.

t-p combinations	β_{21}	β_{22}	β_{31}	β_{32}	β_{41}	β_{42}
^{6}Li + ^{296}Ts	−0.035	−0.099	0.00	0.00	−0.008	0.00
^{18}C + ^{284}Fl	0.062	−0.353	0.00	0.00	0.010	0.00
^{27}Al + ^{275}Bh	0.164	−0.448	0.00	0.00	−0.063	0.239
^{35}Cl + ^{267}Lr	0.22	−0.252	0.00	0.00	−0.064	−0.155
^{54}K + ^{248}Md	0.235	−0.373	0.00	0.00	0.049	−0.080
^{92}Sr + ^{210}Pb	0.00	0.08	0.00	0.00	0.008	0.002
^{136}Xe + ^{166}Dy	0.293	0.00	0.00	0.00	0.010	0.000

value. The $\ell_{\max}$ acquired the value $180\hbar$, i.e., in Fig. 4, the point where both the curves of ERs and ff intersect each other or the point where ERs falls down and ff increases. Figure 5 explains that the $1n$ channel has the largest penetrability as compared to other three LPs (light particles), i.e., $2n$, $3n$, and $4n$. The point here to note about $4n$ is that at all E^*'s we got either ^{4}H, ^{4}He, or ^{4}Li instead of $4n$, so we have replaced the binding energies of ^{4}H, ^{4}He, or ^{4}Li with the binding energy of $4n$. The maximum yield P_0 is obtained for the measured asymmetric fission ($A/2 \pm 20$) and for unobserved light particles ($A \leqslant 4$). In this work, we do not have experimental data for evaporation residues (ERs), so we have shown our DCM-predicted numbers. According to that in ERs, $1n$ has the higher P_0 at all energies, and in the case of fission ^{96}Sr, ^{136}Xe, ^{166}Dy, and ^{210}Pb are at higher values (as shown in Fig. 6). In the DCM, P_0 is a statistical quantity describing the structure of a compound nucleus via decay fragments and this graph also shows the asymmetrical distribution of decay fragments. We have calculated the cross section for $\sigma_{\rm ff}$ and $\sigma_{\rm qf}$ at all given energies at different value of ΔR under the limitations of preformation probability; i.e., P_0 should not be unity. Figure 6 shows the preformation probability with regard to fragment mass number for Ni-induced reaction and also gives the information regarding the most probable fragments which are lying on the top of the preformation probability and same decay fragments are lying at the minima in Fig. 3 (for Ni-induced reaction). This figure shows the asymmetric fission minimum (or peaks) at the magic $N = {}^{136}$Xe (and ^{166}Dy), the qf peaks at ^{94}Sr (and naturally occurring radioactive nuclide element of the uranium (^{238}U) radioactive series ^{210}Pb), and the other intermediate mass fragments (IMFs) minima (peaks) at ^{54}K which occur in weakly bound neutron-rich light nuclei. In this work, the calculated value of ΔR for unobserved decay channel is the same at all energies. This refers to the observation taken from the result for the prediction of ERs in the case of $Z = 122$.

Table II presents the DCM-calculated fission ($\sigma_{\rm ff}^{\rm Cal.}$) and quasifission cross section ($\sigma_{\rm qf}^{\rm Cal.}$) and also predicts the unobserved cross section for ERs, i.e., $\sigma_{\rm ER}^{\rm predicted}$ for the case $\Phi_c = 0^\circ$. Earlier calculations for $Z = 122$ [5] using $\Phi = 0^\circ$ configuration, included higher multipole deformations $\beta_{\lambda i}$ ($\lambda = 2, 3, 4$; $i = 1, 2$), and compact orientations $\theta_{\rm ci}$, has similar experimental data as we have in $Z = 120$ but only at one E^*. The order of DCM-predicted cross section for evaporation residues in both cases ($Z = 120$ and 122) is almost the same (of the order of pb). Figure 7 shows the variations of DCM-calculated $\sigma_{\rm ff}$, $\sigma_{\rm qf}$ with regard to the experimental data. $\sigma_{\rm ff}$ and $\sigma_{\rm qf}$ are increasing functions of E^* as shown in the figure. In our calculations, we have shown that the evaporation residues have very small magnitudes of the order of 10^{-16}, 10^{-22}, 10^{-20}, and 10^{-8} pb, which is a very small cross section, and after the calculation of $P_{\rm CN}$ it seems that the ^{64}Ni-induced reaction does not provide a good option to synthesize $Z = 120$ nuclei. The survival probability is zero in this case, only because of the very small order of evaporation

TABLE II. DCM-calculated fission (ff = $A/2 \pm 20$) and quasifission cross sections compared with experimental data (Ref. [1]) for ^{64}Ni + ^{238}U reaction for best fitted ΔR, also gives DCM-predicted and estimated cross sections for unobserved evaporation residues (ERs), with the included quadrupole deformations only for $\Phi_c = 0^\circ$. The $\sigma_{\rm qf}^{\rm Cal.}$ has been calculated for the entrance channel alone and for ER cross sections; only the $1n$ decay channel is found to contribute. The CN formation probability PCN $\ll 1$, i.e., 0.02, 0.03, 0.04, 0.01 at $E^* = 62$, 43, 31, and 19 MeV respectively and survival probability $P_{\rm surv} \longrightarrow 0$ because ER is in pb, ff, and qf are in mb.

E^*	$\sigma_{xn}^{\rm predicted/estimated}$ $\Delta R_{\rm ER} = -0.25$ fm				$\sigma_{\rm ER} \equiv \sigma_{1n}$	$\Delta R_{\rm ff}$	$\sigma_{\rm ff}^{\rm Cal.}$	$\sigma_{\rm ff}^{\rm Expt.}$	ΔR_{qf}	$\sigma_{qf}^{\rm Cal.}$	$\sigma_{qf}^{\rm Expt.}$
MeV	$1n$	$2n$	$3n$	$4n$	(pb)	fm	(mb)	(mb)	fm	(mb)	(mb)
62	1.698×10^{-16}	3.661×10^{-22}	6.54×10^{-36}	1.418×10^{-30}	1.698×10^{-16}	0.108	3.01	3.097	1.069	126	125.9
43	2.936×10^{-13}	2.932×10^{-18}	1.273×10^{-22}	3.989×10^{-26}	2.936×10^{-22}	0.060	0.699	0.692	0.9425	34.2	34.307
31	1.079×10^{-08}	1.038×10^{-12}	1.514×10^{-16}	8.843×10^{-20}	1.079×10^{-08}	0.467	0.0801	0.0805	0.765	3.56	3.564
19	2.161×10^{-20}	2.405×10^{-27}	3.0795×10^{-33}	1.178×10^{-37}	2.161×10^{-20}	0.2434	0.00467	0.00470	0.7639	0.927	0.9289

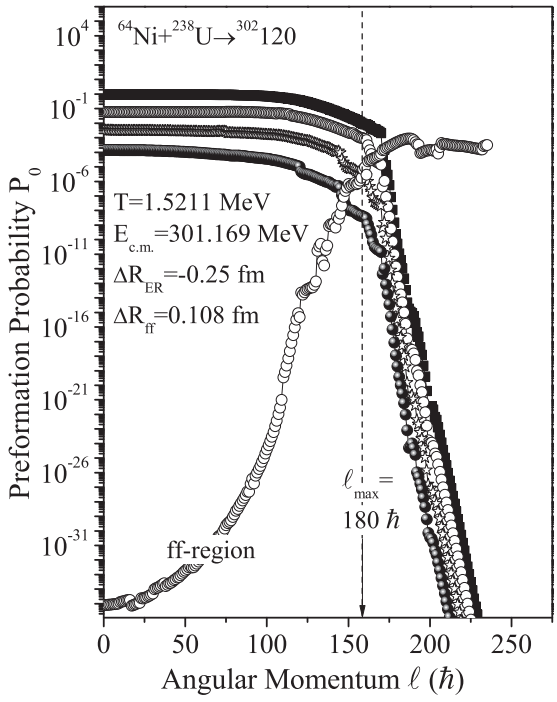

FIG. 4. Preformation probability P_0 for the compound system $Z = 120$ at best fitted ΔR's, calculated for optimum orientations at maximum angular momentum $\ell_{\max} = 180$. For the light fragment mass region ($A_2 = 1$–$4n$) $\Delta R = -0.25$ fm and for fission region ($A/2 \pm 20 = 123$–142) $\Delta R = 0.108$ fm. Here, the curves from both regions intersect each other at a common point where ER's cross section falls down and ff cross section goes high that value is $\ell_{\max}$ in the case of SHEs.

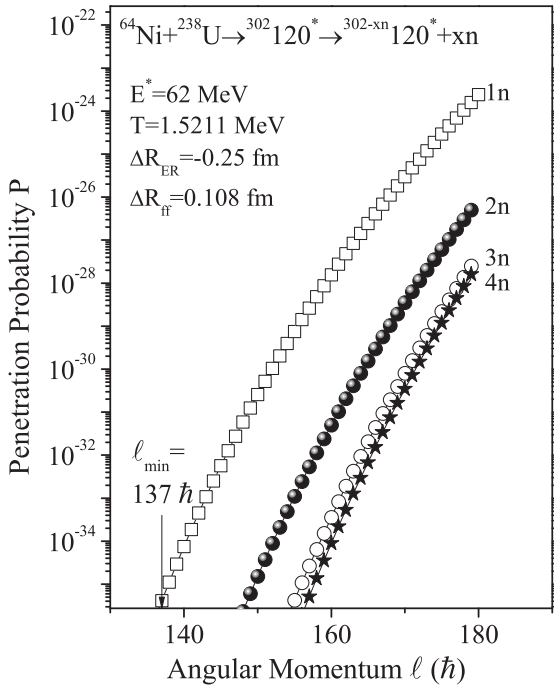

FIG. 5. Same as for Fig. 4, but for penetrability P. $P \approx 10^{-10}$ for $\ell_{\min} = 137\ \hbar$.

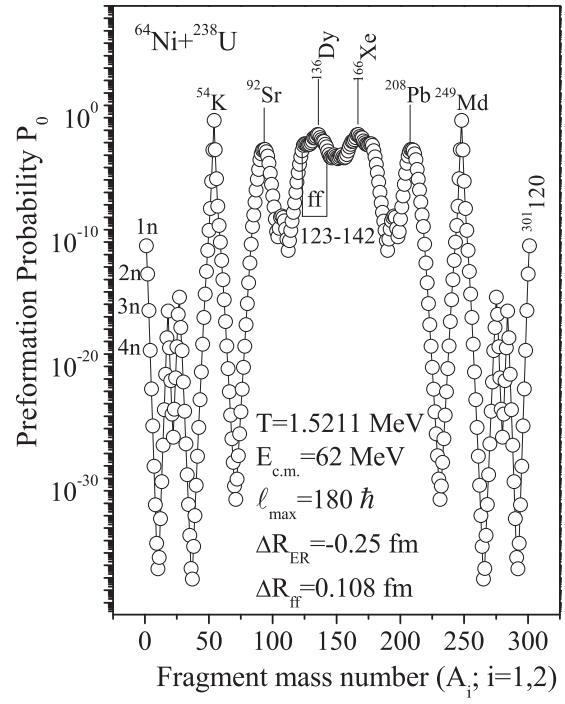

FIG. 6. Preformation probability P_0 as a function of fragment mass number for the decay of $^{302}120^{*}$ formed in $^{64}\mathrm{Ni} + {}^{132}\mathrm{U}$ reaction at $E_{\mathrm{c.m.}} = 301.169$ MeV and at $\ell_{\max} = 180\hbar$ values.

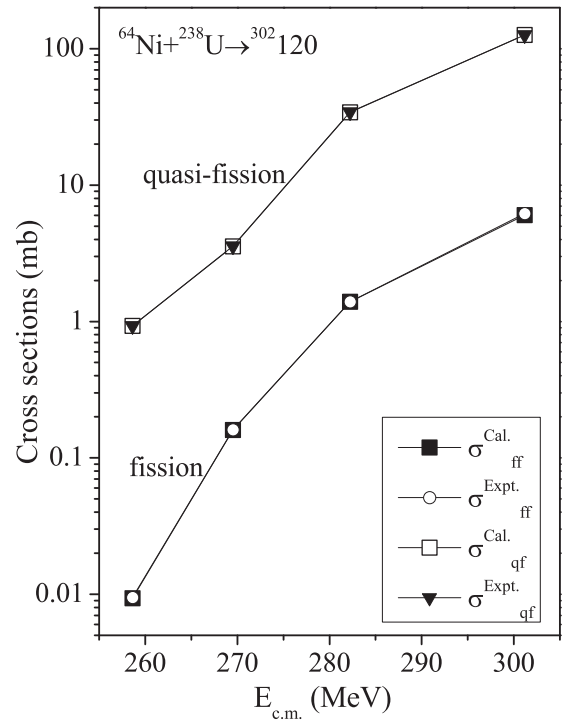

FIG. 7. The DCM-calculated σ_{ff} and σ_{qf} for $^{64}\mathrm{Ni} + {}^{238}\mathrm{U} \rightarrow {}^{302}120^{*}$ reaction, using $\Phi = 0^{\circ}$ case with θ_{ci} and higher multipole deformations β_2–β_4, plotted as a function of $E_{\mathrm{c.m.}}$, compared with experimental data.

TABLE III. DCM-calculated estimated and predicted cross sections [2] for $^{48}Cr + ^{238}Cm$ reaction for best fitted ΔR, also gives DCM-predicted and estimated cross sections for unobserved evaporation residues (ERs), with the included higher multipole deformations only for $\Phi_c = 0^\circ$. Only the $1n$ decay channel is found to contribute. The CN formation probability PCN $\ll 1$ and survival probability $P_{\rm surv} \longrightarrow 0$ because ER is in pb and ff is in mb.

$^{48}Cr + ^{238}Cm$ decay channels	ΔR	Cross section (pb)
$1n$	0.2	1.833×10^{-12}
$2n$	0.2	8.415×10^{-18}
$3n$	1.3854	0.58
$4n$	1.009	1.343×10^{-10}
predicted ff	0.5	3.54 (mb)

residues. Therefore, this is another reason to discard this incoming channel for the synthesis of $Z = 120$. Another point of interest in this calculation is the neck-length parameter (ΔR) for the evaporation residues ($1n$, $2n$, $3n$, and $4n$), i,e., exactly the same at all energies ($\Delta R_{\rm ER}s = -0.25$ MeV).

Figure 8 depicts the results for the P_0 with regard to angular momentum of the $^{54}Cr + ^{248}Cm$ reaction Ref. [2], which was discussed experimentally only at one energy. According to our DCM-calculated values (see Table III), we have tried to explore the possibility for $\sigma_{\rm ER}$ and $\sigma_{\rm ff}$; therefore both are not experimentally given. Figure 8 explains the preformation probability of $^{302}120$ via this incoming channel. The decay

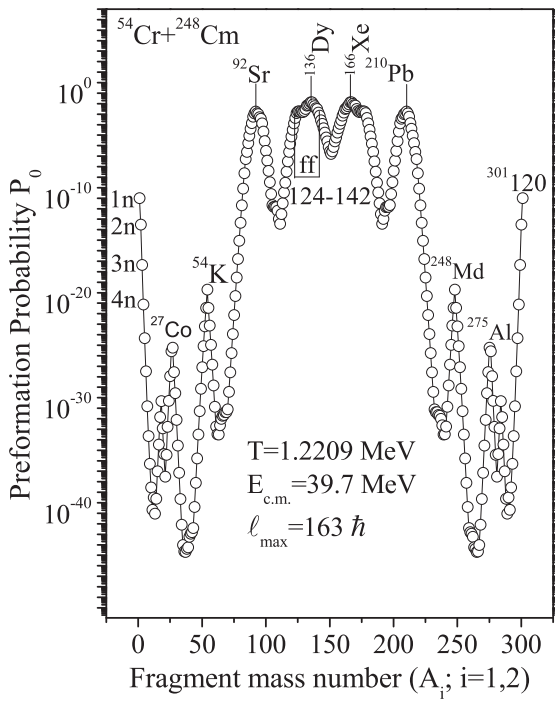

FIG. 8. Preformation probability P_0 as a function of fragment mass number for the decay of $^{302}120^*$ formed in $^{54}Cr + ^{248}Cm$ reaction at $E^* = 39.7$ MeV and at $\ell_{\rm max} = 163\hbar$ values.

fragments from Ni-induced and Cr-induced reaction is nearly the same at the peaks but E^* is different for both. Finally, we have estimated the unobserved *ERs* cross section in the chosen reaction at all energies where only $\sigma_{\rm ff}$ and $\sigma_{\rm qf}$ are given. Further, interesting results of the DCM predictions are that, in agreement with experiments, the asymmetric fission maxima (in the observed ff mass region of $A/2 \pm 20$) lie at the magic $N = 82$, ^{136}Xe (and ^{166}Dy), and the qf peaks at ^{92}Sr (and at ^{210}Pb). In our previous publications [5,7], we have shown the ability of the neck-length parameter for the unobserved decay fragments. We have calculated the estimated and predicted cross sections for ERs.

IV. SUMMARY AND CONCLUSIONS

Summarizing, in this paper, we have analyzed $\sigma_{\rm ff}$ and $\sigma_{\rm qf}$, and both are in good agreement with the experimental data. At all energies, we have estimated and predicted cross sections for the evaporation residues (ERs); their magnitude is very small, of the order of picobarn (pb). The fusion probability is negligible so the nuclear system prefers to proceed via quasifission. Therefore, due to very small evaporation residues cross section, the fusion probability ($P_{\rm CN}$) is negligible so there are more chances for a nuclear system to decay via quasifission. In this work, we have considerable points to explore the possibility of formation of $Z = 120$. On the bases of our DCM calculations, the $^{64}Ni + ^{238}U$ incoming channel seems inappropriate for the formation of $Z = 120$. The estimated and predicted cross sections for evaporation residues (ERs) are largest for the $1n$ decay channel, whereas in the case of $Z = 122$ the contribution of the $4n$ decay channel is largest. In the case of $Z = 122$, we have taken intentionally the neck-length parameter (ΔR) as the same for ERs at all energies, but in this case for $Z = 120$, naturally we got the same ΔR for ERs. This statement makes our work more authentic, which can be taken seriously for further experiments after verification, which will help us to settle our theoretical results.

ACKNOWLEDGMENTS

This work was supported by the department of Physics, Panjab University, Chandigarh. P.O.H. acknowledges financial support from "Direccion General de Asuntos del Personal Academico UNAM", PAPIIT-DGAPA (IN100421). We also gratefully acknowledge the well-informed discussions with Horst Stoecker from Frankfurt Institute for Advanced Studies, J.W. von Goethe-University, Frankfurt, and Sophia Heinz from GSI Helmholtzzentrum für Schwerionenforschung, Darmstadt, Germany, and especially we would like to show our gratitude to the late Prof. Emeritus Dr. R. K. Gupta for his advice and support to start this work under his guidance.

[1] E. M. Kozulin, G. N. Knyazheva, I. M. Itkis, M. G. Itkis, A. A. Bogachev, L. Krupa, T. A. Loktev, S. V. Smirnov, V. I. Zagrebaev, J. Åystö *et al.*, Phys. Lett. B **686**, 227 (2010).

[2] S. Hofmann, S. Heinz, R. Mann, J. Maurer, G. Münzenberg, S. Antalic, W. Barth, H. G. Burkhard, L. Dahl, K. Eberhardt *et al.*, Eur. Phys. J. A **52**, 180 (2016).

[3] R. K. Gupta, S. K. Arun, R. Kumar, and Niyti, Int. Rev. Phys. **2**, 369 (2008).

[4] R. K. Gupta, in *Clusters in Nuclei*, Lecture Notes in Physics Vol. 818, edited by C. Beck (Springer Verlag, Berlin, 2010), Vol. I, pp. 223–265; and earlier references therein.

[5] S. Chopra, Hemdeep, and R. K. Gupta, Phys. Rev. C **95**, 044603 (2017).

[6] S. K. Arun, R. Kumar, and R. K. Gupta, J. Phys. G: Nucl. Part. Phys. **36**, 085105 (2009).

[7] S. Chopra, M. K. Sharma, P. O. Hess *et al.*, Phys. Rev. C **103**, 064615 (2021).

[8] R. K. Gupta, N. Singh, and M. Manhas, Phys. Rev. C **70**, 034608 (2004).

[9] J. Maruhn and W. Greiner, Phys. Rev. Lett. **32**, 548 (1974).

[10] R. K. Gupta, W. Scheid, and W. Greiner, Phys. Rev. Lett. **35**, 353 (1975).

[11] D. R. Saroha and R. K. Gupta, J. Phys. G: Nucl. Phys. **12**, 1265 (1986).

[12] R. K. Gupta, N. Malhotra, and D. R. Saroha, α-clustering in 75 MeV $^{16}O^{*} + {}^{40}Ca^{*}$ as a collective mass fragmentation process. Report No. IC/85/74, ICTP, Trieste, Italy, 1985.

[13] H. Kröger and W. Scheid, J. Phys. G **6**, L85 (1980).

[14] D. R. Inglis, Phys. Rev. **96**, 1059 (1954).

[15] S. T. Balyaev, K. Dan. Vidensk. Selsk. Mat.-Fys. Medd. **31**, 11 (1959).

[16] N. J. Davidson, S. S. Hsiao, J. Markram, H. G. Miller, and Y. Tzeng, Nucl. Phys. A **570**, 61c (1994).

[17] B. B. Singh, M. K. Sharma, and R. K. Gupta, Phys. Rev. C **77**, 054613 (2008).

[18] R. K. Gupta, R. Kumar, N. K. Dhiman, M. Balasubramaniam, W. Scheid, and C. Beck, Phys. Rev. C **68**, 014610 (2003).

[19] M. Balasubramaniam, R. Kumar, R. K. Gupta, C. Beck, and W. Scheid, J. Phys. G: Nucl. Part. Phys. **29**, 2703 (2003).

[20] G. Audi, A. H. Wapstra, and C. Thiboult, Nucl. Phys. A **729**, 337 (2003).

[21] W. Myers and W. J. Swiatecki, Nucl. Phys. **81**, 1 (1966).

[22] J. Blocki, J. Randrup, W. J. Swiatecki, and C. F. Tsang, Ann. Phys. (NY) **105**, 427 (1977).

[23] W. Pauli, in *Handbuck der Physik*, edited by H. Geiger and K. Sheel (Springer, Berlin, 1933), Vol. 24, Part I, p. 120; B. Padolsky, Phys. Rev. **32**, 812 (1928); J. Eisenberg and W. Greiner, *Nuclear Models* (North Holland, Amsterdam, 1971), p. 136.

[24] R. K. Gupta, in *Proceedings of the 5th International Conference on Nuclear Reaction Mechanisms*, edited by E. Gadioli (Ricerca Scintifica Educazione Permanente, Varenna, Italy, 1988), p. 416.

[25] S. S. Malik and R. K. Gupta, Phys. Rev. C **39**, 1992 (1989).

[26] A. Kaur, S. Chopra, and R. K. Gupta, Phys. Rev. C **90**, 024619 (2014).

[27] S. Chopra, A. Kaur, and R. K. Gupta, Phys. Rev. C **91**, 034613 (2015).

[28] G. Royer and J. Mignen, J. Phys. G: Nucl. Part. Phys. **18**, 1781 (1992).

[29] H. S. Khosla, S. S. Malik, and R. K. Gupta, Nucl. Phys. A **513**, 115 (1990).

[30] S. Kumar and R. K. Gupta, Phys. Rev. C **55**, 218 (1997).

[31] R. K. Gupta, S. Kumar, and W. Scheid, Int. J Mod. Phys. E **6**, 259 (1997).